

# Single production of the top partners at high energy colliders

Chong-Xing Yue, Hui-Di Yang, Wei Ma

Department of Physics, Liaoning Normal University, Dalian 116029, P. R. China \*

March 23, 2009

## Abstract

The left-right twin *Higgs* (*LRTH*) model is a concrete realization of the twin *Higgs* mechanism, which predicts the existence of the top partner  $T$ . In this paper, we consider production of  $T$  associated with the top quark  $t$  at the high energy linear  $e^+e^-$  collider (*ILC*) and the *LHC* experiments, and its single production in future linac-ring type  $ep$  collider experiment. To compare our results with those of the littlest *Higgs* model with  $T$ -parity, we also estimate production of the  $T$ -even top partner  $T_+$  via the corresponding processes in these high energy collider experiments. A simply phenomenological analysis is also given.

---

\*E-mail:cxyue@lnnu.edu.cn

## 1. Introduction

Although the standard model ( $SM$ ) of elementary particle physics provides a very successful description of existing experiments at the highest energies currently accessible at colliders, there is the fine tuning problem to be solved in the  $SM$ . To solve the fine tuning problem, many new physics models beyond the  $SM$  have been proposed. However, a so-called "little hierarchy problem" [1] arises in these models, once constraints from precision measurements are imposed. So far, there are some successful models solving the little hierarchy problem, for example the  $MSSM$  with  $R$ -parity [2], the little *Higgs* models [3], the universal extra dimensional model with  $KK$ -parity [4], or the twin *Higgs* mechanism [5].

It is well known that the top loop in the  $SM$  is the largest contribution to the *Higgs* mass quadratic divergence. Thus, for the new physics models to solve the fine tuning problem, there must be some particles constrained by symmetry, which cancel this loop. All of the models mentioned above contain a heavy particle which shares the gauge quantum numbers of the top quark, generally called "top partner" [6]. This kind of new particles can lead to a relatively generic class of collider signals from their production and subsequent decay, which have been extensively studied in the literature [7, 8, 9].

Recently, the twin *Higgs* mechanism has been proposed as a solution to the little hierarchy problem [5]. The twin *Higgs* mechanism proceeds in two main steps: i) the  $SM$  *Higgs* emerges as a pseudo-*Goldstone* boson from a spontaneously broken global symmetry; ii) an additional discrete symmetry is imposed, which can make that the leading quadratically divergent terms cancel each other and do not contribute the *Higgs* mass. The twin *Higgs* mechanism can be implemented in left-right models with the additional discrete symmetry being identified with left-right symmetry [10, 11]. The left-right twin *Higgs* ( $LRTH$ ) model contains the  $U(4)_1 \times U(4)_2$  global symmetry as well as the gauged symmetry  $SU(2)_L \times SU(2)_R \times U(1)_{B-L}$ . After *Higgs* obtain vacuum expectation values, the global symmetry  $U(4)_1 \times U(4)_2$  breaks down to  $U(3)_1 \times U(3)_2$ , and the gauge group  $SU(2)_R \times U(1)_{B-L}$  breaks down to the  $SM$   $U(1)_Y$ . The leading quadratically divergent contributions of the  $SM$  gauge bosons to the *Higgs* mass are

canceled by the loop involving the new gauge bosons, while those for the top quark can be canceled by the contributions from a heavy top quark called top partner. Thus, the *LRTH* model predicts the existence of the new particles, such as heavy gauge bosons, heavy scalars, and the top partner, which can generate rich phenomenology at present and in future collider experiments [11, 12, 13, 14].

The single and pair production of the top partners predicted by the *LRTH* model at the *LHC* are studied in Ref. [11]. As we know, so far, in the context of the *LRTH* model, production of the top partner associated with the top quark  $t$  has not been considered at the high energy linear  $e^+e^-$  collider (*ILC*), the linac-ring type  $ep$  collider (*THERA*), and the *LHC*, which is the main aim of this paper. There are several motivations to perform this study. First, so far, most of works about the top partner focus on phenomenology analysis at the *LHC*. Studies about production of the top partner at *ILC* and *THERA* are very few. Second, the top partner predicted by different new physics models might generate similar signatures at the *LHC*. It is very difficult to differentiate each other. Third, as long as the top partner is not too heavy, it can be singly produced in future *ILC* and *THERA* experiments. These high energy collider experiments with more clear environment could help us to distinguish different new physics models. Thus, in this paper, we will completely consider single production of the top partner in these three kinds of the high energy collider experiments and compare the numerical results with each other.

The layout of the present paper is as follows: In section 2, we briefly review the essential features of the *LRTH* model. The relevant couplings of the top partner  $T$  to other particles are also given in this section. Single production of  $T$  in future *ILC*, *THERA*, and *LHC* experiments are calculated in sections 3, 4, and 5, respectively. In these sections, we discuss the possible signals generated by the processes  $e^+e^- \rightarrow t\bar{T} + \bar{t}T$ ,  $ep \rightarrow \nu_e\bar{T} + X$ , and  $pp \rightarrow t\bar{T} + \bar{t}T + X$ . To compare our results obtained in the context of the *LRTH* model with those of the littlest *Higgs* model with  $T$ -parity, called the *LHT* model [15], we further consider production of the  $T$ -even top partner  $T_+$  via the corresponding processes in these three sections. Finally, our conclusions are given in

section 6.

## 2. The *LRTH* model

The *LRTH* model was first proposed in Ref. [10] and the details of the model as well as the particle spectrum, *Feynman* rules, and some phenomenology analysis have been studied in Ref. [11]. Here we will briefly review the essential features of the model and focus our attention on the heavy gauge bosons and heavy top partner.

The *LRTH* model is based on the global  $U(4)_1 \times U(4)_2$  symmetry with a locally gauged subgroup  $SU(2)_L \times SU(2)_R \times U(1)_{B-L}$ . Two *Higgs* fields,  $H = (H_L, H_R)$  and  $\hat{H} = (\hat{H}_L, \hat{H}_R)$ , are introduced and each transforms as  $(4, 1)$  and  $(1, 4)$  respectively under the global symmetry.  $H_{L,R}$  ( $\hat{H}_{L,R}$ ) are two component objects which are charged under  $SU(2)_L$  and  $SU(2)_R$ , respectively. For the gauge couplings  $g_{2L}$  and  $g_{2R}$  of  $SU(2)_L$  and  $SU(2)_R$ , the left-right symmetry implies that  $g_{2L} = g_{2R} = g_2$ .

The  $U(4)_1$  ( $U(4)_2$ ) group is spontaneously broken down to its subgroup  $U(3)_1$  ( $U(3)_2$ ) with non-zero vacuum expectation value (*VEV*)  $\langle H \rangle = (0, 0, 0, f)$  ( $\langle \hat{H} \rangle = (0, 0, 0, \hat{f})$ ). The *Higgs VEVs* also break  $SU(2)_R \times U(1)_{B-L}$  down to the *SM*  $U(1)_Y$ . After spontaneous global symmetry breaking by  $f$  and  $\hat{f}$ , three *Goldstone* bosons are eaten by the new gauge bosons  $W_H^\pm$  and  $Z_H$ . After the electroweak symmetry breaking, the three additional *Goldstone* bosons are eaten by the *SM* gauge bosons  $W^\pm$  and  $Z$ . In the *LRTH* model, the masses of the heavy gauge bosons can be written as:

$$M_{W_H}^2 = \frac{1}{2}g_2^2(\hat{f}^2 + f^2 \cos^2 x), \quad (1)$$

$$M_{Z_H}^2 = \frac{g_1^2 + g_2^2}{g_2^2}(M_{W_H}^2 + M_W^2) - M_Z^2, \quad (2)$$

where  $x = v/\sqrt{2}f$ .  $g_1$  and  $g_2$  ( $= g_{2L} = g_{2R}$ ) are the gauge coupling constants of the  $U(1)_{B-L}$  and  $SU(2)_{L,R}$ , respectively, which can be written as:

$$g_1 = \frac{e}{\sqrt{\cos 2\theta_W}}, \quad g_2 = \frac{e}{S_W}. \quad (3)$$

Where  $S_W = \sin \theta_W$  and  $\theta_W$  is the *Weinberg* angle.

The fermion sector of the *LRTH* model is similar to that of the *SM*, with the right handed quarks  $(u_R, d_R)$  and leptons  $(l_R, \nu_R)$  form fundamental representations of  $SU(2)_R$ .

In order to give the top quark mass of the order of the electroweak scale, a pair of vector-like quarks  $Q_L$  and  $Q_R$  are introduced. The mass eigenstates, which contain one the  $SM$  top quark  $t$  and a heavy top partner  $T$ , are mixtures of the gauge eigenstates. Their masses are given by

$$m_t^2 = \frac{1}{2}(M^2 + y^2 f^2 - N_t), \quad M_T^2 = \frac{1}{2}(M^2 + y^2 f^2 + N_t), \quad (4)$$

where  $N_t = \sqrt{(y^2 f^2 + M^2)^2 - y^4 f^4 \sin^2 2x}$ . Provided  $M_T \leq f$  and that the parameter  $y$  is of order one, the top *Yukawa* coupling will also be of order one. The parameter  $M$  is essential to the mixing between the  $SM$  top quark and its partner. At the leading order of  $1/f$ , the mixing angles can be written as:

$$S_L = \sin \alpha_L \simeq \frac{M}{M_T} \sin x, \quad S_R = \sin \alpha_R \simeq \frac{M}{M_T} (1 + \sin^2 x). \quad (5)$$

The left(right) coupling constants of the gauge bosons and the top partner  $T$  to other particles, which are related our calculation, can be written as:

$$g_L^{Zt\bar{T}} = \frac{eC_L S_L}{2C_W S_W}, \quad g_R^{Zt\bar{T}} = \frac{ef^2 x^2 S_W C_R S_R}{2\hat{f}^2 C_W^3}; \quad (6)$$

$$g_L^{Ze^+e^-} = \frac{e(-\frac{1}{2} + S_W^2)}{S_W C_W}, \quad g_R^{Ze^+e^-} = \frac{eS_W}{C_W}; \quad (7)$$

$$g_L^{Z_H t\bar{T}} = \frac{eC_L S_L S_W}{2C_W \sqrt{\cos 2\theta_W}}, \quad g_R^{Z_H t\bar{T}} = -\frac{eC_R S_R C_W}{2S_W \sqrt{\cos 2\theta_W}}; \quad (8)$$

$$g_L^{Z_H e^+e^-} = \frac{2eS_W}{4C_W \sqrt{\cos 2\theta_W}}, \quad g_R^{Z_H e^+e^-} = \frac{e(1 - 3 \cos 2\theta_W)}{4S_W C_W \sqrt{\cos 2\theta_W}}; \quad (9)$$

$$g_L^{W\bar{T}b} = \frac{eS_L}{\sqrt{2}S_W}, \quad g_L^{W\nu_e e} = \frac{e}{\sqrt{2}S_W}; \quad (10)$$

$$g_R^{W_H \bar{T}b} = \frac{eC_R}{\sqrt{2}S_W}, \quad g_R^{W_H \nu_e e} = \frac{e}{\sqrt{2}S_W}. \quad (11)$$

Where  $C_L^2 = 1 - S_L^2$ ,  $C_R^2 = 1 - S_R^2$ .

According to the symmetry breaking pattern discussed above, with certain reparametrization of the fields, there are left with four scalars in the  $LRT H$  spectrum that couple to both the fermion sector and the gauge boson sector. They are one neutral pseudo scalar  $\phi^0$ , a pair of charged scalars  $\phi^\pm$ , and the  $SM$  physical *Higgs*  $h$ . In addition, there is an  $SU(2)_L$  doublet  $\hat{h} = (\hat{h}_1^+, \hat{h}_2^0)$  that couples to the gauge boson sector only. It has been shown that the lightest particle in  $\hat{h}$ , typically one of the neutral components, is stable, and therefore constitutes a good dark matter candidate [14]. Thus, the top quark  $t$  and its partner  $T$  can couple to some of these scalars:

$$ht\bar{t} : -\frac{e}{2S_W} \frac{m_t C_L C_R}{m_W}, \quad hT\bar{T} : -\frac{y}{\sqrt{2}}(S_R S_L - C_L C_R x); \quad (12)$$

$$\phi^0 t\bar{t} : -\frac{iy}{\sqrt{2}} S_R S_L, \quad \phi^0 T\bar{T} : -\frac{iy}{\sqrt{2}} C_L C_R; \quad (13)$$

$$h\bar{T}t : -\frac{y}{\sqrt{2}}[(C_L S_R + S_L C_R x)P_L + (C_L S_R x + S_L C_R)P_R]; \quad (14)$$

$$\phi^0 \bar{T}t : -\frac{iy}{\sqrt{2}}[S_L C_R P_L - C_L S_R P_R], \quad \phi^+ \bar{T}b : \frac{i}{f}[C_R m_b P_L - y C_L f P_R]. \quad (15)$$

Thus, the possible decay modes of the top partner  $T$  are  $\phi^+ b$ ,  $W^+ b$ ,  $th$ ,  $tZ$ , and  $t\phi^0$ , which are extensively studied in Ref. [11].

In the following sections, we will use the above *Feynman* rules to calculate the single production cross sections of the top partner  $T$  and discuss its possible signals at the *ILC*, *THERA*, and *LHC* experiments.

### 3. Production of the top partner $T$ associated with the top quark $t$ at the *ILC*

From the above discussions, we can see that production of the top partner  $T$  associated with the top quark  $t$  via  $e^+e^-$  collision proceeds through the  $S$ -channel  $Z$  exchange and  $Z_H$  exchange as shown in Fig.1. Using Eqs.(6)-(9), the production cross section  $\sigma_1$  can be written as:

$$\sigma_1(s) = \frac{3\sqrt{(s + M_T^2 - m_t^2)^2 - 4sM_T^2}}{8\pi s^2} \left\{ \frac{((g_L^{Ze^+e^-})^2 + (g_R^{Ze^+e^-})^2)((g_L^{Zt\bar{T}})^2 + (g_R^{Zt\bar{T}})^2)}{2(s - M_Z^2)^2} \right\}$$

$$\begin{aligned}
& + \frac{((g_L^{Z_H e^+ e^-})^2 + (g_R^{Z_H e^+ e^-})^2)((g_L^{Z_H t \bar{T}})^2 + (g_R^{Z_H t \bar{T}})^2)}{2(s - M_{Z_H}^2)^2} \\
& + \frac{(g_L^{Z e^+ e^-} g_L^{Z_H e^+ e^-} + g_R^{Z e^+ e^-} g_R^{Z_H e^+ e^-})(g_L^{Z t \bar{T}} g_L^{Z_H t \bar{T}} + g_R^{Z t \bar{T}} g_R^{Z_H t \bar{T}})}{(s - M_Z^2)(s - M_{Z_H}^2)}] \\
& \left( \frac{s^2 - (M_T^2 - m_t^2)^2}{4} + \frac{(s + M_T^2 - m_t^2)^2 - 4sM_T^2}{12} \right) \\
& + \left[ \frac{g_R^{Z t \bar{T}} g_L^{Z t \bar{T}} ((g_L^{Z e^+ e^-})^2 + (g_R^{Z e^+ e^-})^2)}{(s - M_Z^2)^2} + \frac{g_R^{Z_H t \bar{T}} g_L^{Z_H t \bar{T}} ((g_L^{Z_H e^+ e^-})^2 + (g_R^{Z_H e^+ e^-})^2)}{(s - M_{Z_H}^2)^2} \right. \\
& \left. + \frac{(g_L^{Z e^+ e^-} g_L^{Z_H e^+ e^-} + g_R^{Z e^+ e^-} g_R^{Z_H e^+ e^-})(g_R^{Z t \bar{T}} g_L^{Z_H t \bar{T}} + g_L^{Z t \bar{T}} g_R^{Z_H t \bar{T}})}{(s - M_Z^2)(s - M_{Z_H}^2)} \right] m_t M_T s \}. \quad (16)
\end{aligned}$$

Where  $\sqrt{s}$  is the center-of-mass (*c.m.*) energy of the *ILC*.

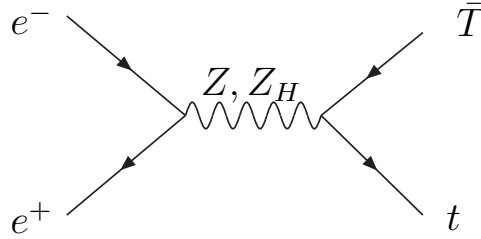


Figure 1: *Feynman* diagrams for the process  $e^+e^- \rightarrow t\bar{T}$  in the *LRTH* model.

From the above expression, we can see that, except for the *SM* input parameters  $\alpha_e = 1/128.8$ ,  $S_W^2 = 0.2315$ ,  $m_t = 172.5 \text{ GeV}$ , and  $M_Z = 91.187 \text{ GeV}$  [16], the production cross section  $\sigma_1$  for the top partner  $T$  at the *ILC* is dependent on the model dependent parameters  $f$ ,  $\hat{f}$ ,  $M$ , and  $M_T$  (or  $y$ ). Once  $f$  is fixed, the scalar *VEV*  $\hat{f}$  can be determined by minimizing the *Coleman – Weinberg* (*CW*) potential for the *SM Higgs* boson and requiring that the *SM Higgs* boson obtains an electroweak symmetry breaking *VEV* of  $246 \text{ GeV}$  [11]. The top *Yukawa* coupling constant  $y$  can be determined by fitting the experimental value of the top mass  $m_t$ . The free parameters  $f$  and  $M$  are constrained by the precision measurements. In our numerical estimation below, we will assume  $M \leq 300 \text{ GeV}$  and  $f \leq 1500 \text{ GeV}$ .

Our numerical results are summarized in Fig.2, in which we plot  $\sigma_1^{LR}$  as a function of the *VEV* value  $f$  for the *c.m.* energy  $\sqrt{s} = 2 \text{ TeV}$  and three values of the mixing

parameter  $M$ . One can see from Fig.2 that the cross section  $\sigma_1^{LR}$  is very sensitive to the parameters  $f$  and  $M$ . When  $M$  inclines to zero, its value goes to zero. This is because  $M = 0$  leads no-mixing between the  $SM$  top and its partner, the  $Zt\bar{T}$  and  $Z_H t\bar{T}$  couplings equal to zero. For  $M = 200 \text{ GeV}$  and  $500 \text{ GeV} \leq f \leq 1200 \text{ GeV}$ , the value of  $\sigma_1$  is in the range of  $9.4 \text{ fb} \sim 4.6 \times 10^{-2} \text{ fb}$ , which can generate several and up to hundreds  $t\bar{T} + \bar{t}T$  events per year at the  $ILC$  with a yearly integrated luminosity  $\mathcal{L} = 100 \text{ fb}^{-1}$ .

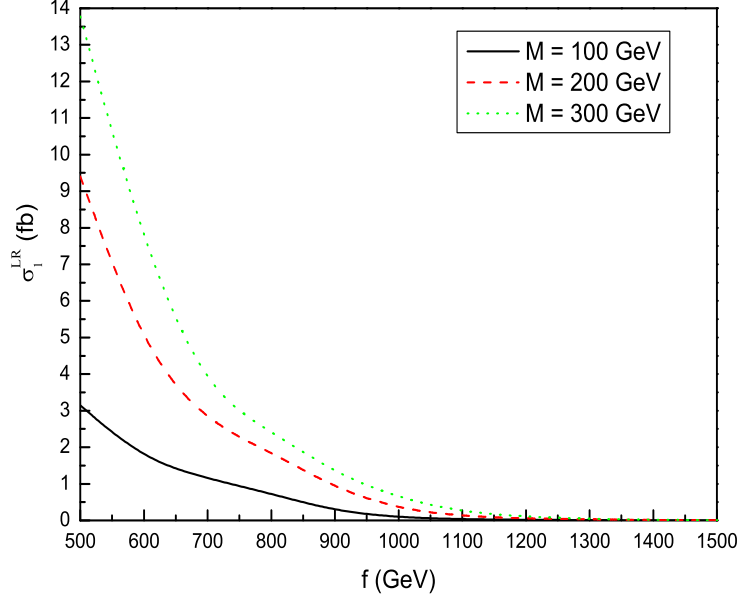


Figure 2: The production cross sections  $\sigma_1^{LR}$  as a function of the  $VEV$  value  $f$  for the  $c.m.$  energy  $\sqrt{s} = 2 \text{ TeV}$  and three values of the mixing parameter  $M$ . We have taken into account both  $T$  and  $\bar{T}$  quarks.

In wide range of the parameter space of the  $L R T H$  model, the possible decay modes of the top partner  $T$  are  $\phi^+ b$ ,  $ht$ ,  $Zt$ ,  $Wb$ , and  $t\phi^0$ . It has been shown that, for  $M = 150 \text{ GeV}$  and  $500 \text{ GeV} \leq f \leq 1500 \text{ GeV}$ , the branching ratio  $Br(T \rightarrow \phi^+ b)$  is larger than 70% and the values for other branching ratios are smaller than 10% [11]. Furthermore, for  $M > 10 \text{ MeV}$ , there is  $Br(\phi^+ \rightarrow t\bar{b}) \simeq 100\%$ . Thus, the dominate decay mode  $\phi^+ b$



makes the process  $e^+e^- \rightarrow t\bar{T} + \bar{t}T$  mainly transfers to the final state  $t\bar{t}b\bar{b}$ . For example, for  $M = 200 \text{ GeV}$ ,  $\sqrt{s} = 2 \text{ TeV}$ , and  $f = 500 \text{ GeV}$ , the production cross section of the final state  $t\bar{t}b\bar{b}$  can reach  $7 \text{ fb}$ . There are two kinds of the main backgrounds for this kind of final state. The first kind is the large  $QCD$  backgrounds, which primarily come from the process  $e^+e^- \rightarrow t\bar{t}g^*$  with the gluon decaying to a  $b\bar{b}$  pair. The second kind is the electroweak backgrounds, of which the dominant contributions induced by the process  $e^+e^- \rightarrow Zt\bar{t}$  with the gauge boson  $Z$  decaying to a  $b\bar{b}$  pair. Considering the leptonic, semileptonic and fully hadronic decays of the  $t\bar{t}$  system, the main background processes  $e^+e^- \rightarrow t\bar{t}g^*$  and  $e^+e^- \rightarrow t\bar{t}Z$  have been extensively studied in the literature [17, 18]. According their conclusions, we have to say that it is very difficult to discriminate the signals generated by the final state  $t\bar{t}b\bar{b}$  from the backgrounds.

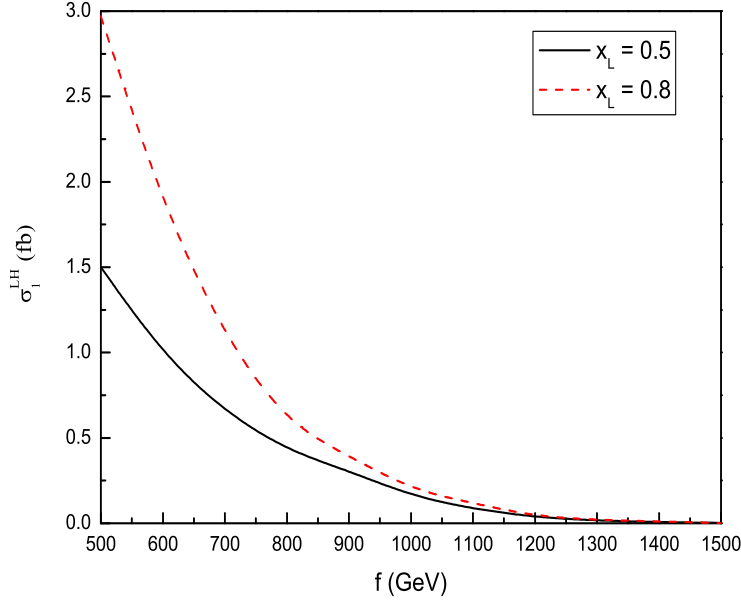


Figure 3: The production cross section  $\sigma_1^{LH}$  as a function of the scale parameter  $f$  for the  $c.m.$  energy  $\sqrt{s} = 2 \text{ TeV}$  and two values of the mixing parameter  $x_L$ . We have taken into account both  $T_+$  and  $\bar{T}_+$  quarks.

The second important decay channel of the top partner  $T$  is  $T \rightarrow W^+b$ . However, it is more difficult to separate the signals generated by the process  $e^+e^- \rightarrow \bar{t}T + t\bar{T}$  with  $T \rightarrow W^+b$  from the large background coming from the  $SM$  process  $e^+e^- \rightarrow t\bar{t}$ . Certainly, the reconstruction of the heavy top partner  $T$  through the combination of  $Wb$  may help to distinguish the signals from the backgrounds. The signals induced by the decay channels  $T \rightarrow th, tZ$ , and  $t\phi_0$ , with  $h \rightarrow b\bar{b}$ ,  $Z \rightarrow b\bar{b}$ , and  $\phi_0 \rightarrow b\bar{b}$  can give rise to similar signals with those of the decay channel  $T \rightarrow \phi^+b$ . However, because of the very small branching ratios, their production rates are much smaller than that of the process  $e^+e^- \rightarrow t\bar{T} + \bar{t}T \rightarrow t\bar{t}b\bar{b}$ .

The littlest *Higgs* model with  $T$ -parity, called the *LHT* model [15], also predicts the existence of the top partner  $T_+$ , which is  $T$ -even and can also be produced in association with the top quark  $t$  via  $e^+e^-$  collision. The *Feynman* diagram is similar with Fig.1. However, the  $T$ -odd gauge boson  $Z_H$  can not contribute the process  $e^+e^- \rightarrow t\bar{T} + \bar{t}T$ . Our numerical results are given in Fig.3, in which we have plotted the production cross section  $\sigma_1^{LH}$  as a function of the scale parameter  $f$  for  $\sqrt{s} = 2 \text{ TeV}$  and two values of the free parameter  $x_L$ . One can see from Fig.3 that, in most of the parameter space, the value of the cross section  $\sigma_1^{LH}$  is smaller than that of the cross section  $\sigma_1^{LR}$ .

The top partner  $T_+$  can decay into  $W^+b$ ,  $Ht$ ,  $Zt$ , and  $B_H t_-$ , in which  $t_-$  is the  $T$ -odd top partner and  $B_H$  is the  $T$ -odd gauge boson. The branching ratios of these decay modes have been estimated in Ref.[19]. The former three decay modes can produce the similar signals to those of the top partner  $T$  predicted by the *LRTH* model. However, their production rates are smaller than the corresponding production rates in the *LRTH* model. In most of the parameter space of the *LHT* model, the  $T$ -odd top partner  $t_-$  mainly decays into  $tB_H$  and there are  $Br(t_- \rightarrow B_H t) \approx 100\%$  [19]. If we assume that  $T$ -parity is strictly conserved, the lightest  $T$ -odd gauge boson  $B_H$  can be seen as an attractive dark matter candidate [20]. Then the  $B_H t_-$  decay mode can give rise to the distinctive state of  $t\bar{t}$  plus large missing energy. The large transverse missing energy can be used to distinguish the signal from the large  $SM$  background  $e^+e^- \rightarrow t\bar{t}$ . However, its production rate is too small to be detected in the future *ILC* experiments. Thus, the

possible signatures of top partner predicted by the *LHT* model or the *LRTH* model all can not be detected via the process  $e^+e^- \rightarrow t\bar{T} + \bar{t}T$  in the future *ILC* experiments.

#### 4. Single production of the top partner $T$ at future $ep$ collider

Although the linac-ring type  $ep$  collider (*THERA*) with the *c.m.* energy  $\sqrt{s} = 3.7$  *TeV* and the integral luminosity  $\mathcal{L} = 100 \text{ pb}^{-1}$ , which is named Energy Frontier  $ep$  collider, has a lower luminosity, it can provide better conditions for studying a lot of phenomena comparing to the *ILC* due to the high center-of-mass energy and to the *LHC* due to more clear environment [21]. Thus, it is very interesting to consider production of the new heavy particles at the *THERA*.

From the discussions given in section 2, we can see that the top partner  $T$  can be singly produced via the process  $ep \rightarrow e\bar{b} + X \rightarrow \nu_e\bar{T} + X$  at the *THERA*. The relevant *Feynman* diagrams are shown in Fig.4. For the subprocess  $e(P_e) + \bar{b}(P_b) \rightarrow \bar{T}(P_T) + \nu_e(P_\nu)$ , we define kinematical invariants  $\hat{s} = (P_e + P_b)^2 = (P_T + P_\nu)^2$  and  $\hat{t} = (P_T - P_b)^2$ . The differential cross section is given by

$$\frac{d\hat{\sigma}_2(\hat{s})}{d\hat{t}} = \frac{\hat{t}^2 + \hat{t}(2\hat{s} - M_T^2) + 2\hat{s}(\hat{s} - M_T^2)}{64\pi\hat{s}^2} \left[ \frac{(g_L^{W\bar{T}b})^2 (g_L^{W\nu_e e})^2}{(\hat{t} - m_W^2)^2} + \frac{(g_R^{W_H\bar{T}b})^2 (g_R^{W_H\nu_e e})^2}{(\hat{t} - m_{W_H}^2)^2} \right]. \quad (17)$$

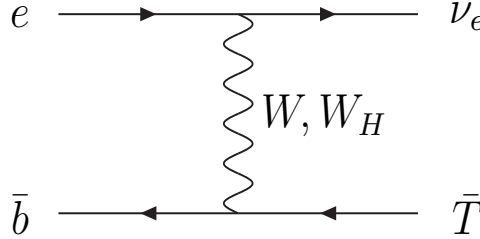


Figure 4: In the *LRTH* model, the *Feynman* diagrams for the subprocess  $e\bar{b} \rightarrow \nu_e\bar{T}$ .

After calculating the cross section  $\hat{\sigma}_2(\hat{s})$  contributed by the  $t$ -channel  $W$  exchange and  $W_H$  exchange, the effective production cross section  $\sigma_2(s)$  can be folding  $\hat{\sigma}_2(\hat{s})$  with the bottom-quark distribution function  $f_b(x)$  in the proton

$$\sigma_2(s) = \int_{x_{min}}^1 f_b(x, \mu_F) \hat{\sigma}_2(\hat{s}) dx \quad (18)$$

with  $x_{min} = M_T^2/s$  and  $\hat{s} = xs$ . In our numerical calculation, we will use *CTEQ6L* parton distribution function [22] for  $f_b(x, \mu_F)$  and assume that the factorization scale  $\mu_F$  is of order  $\sqrt{\hat{s}}$ .

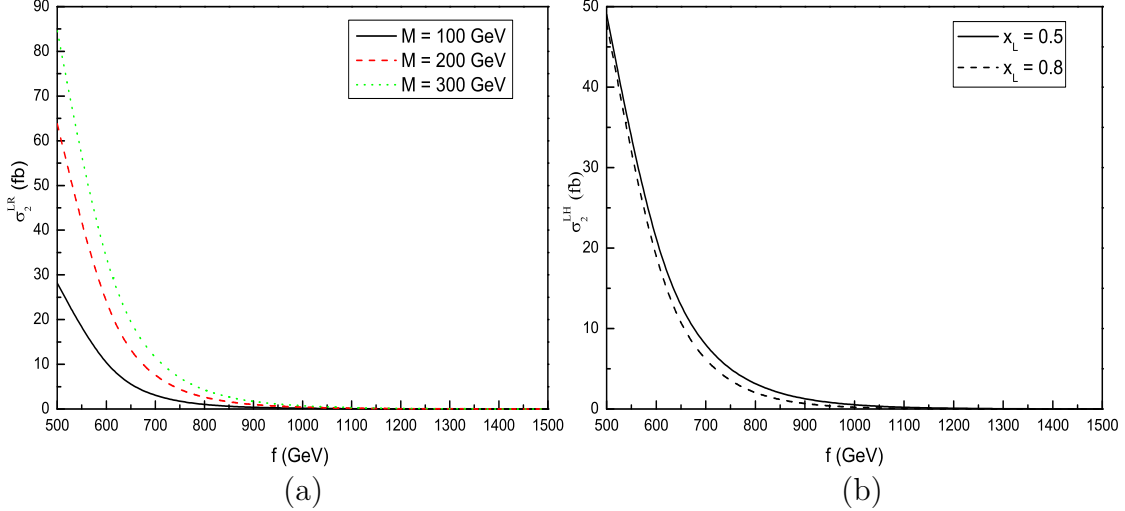


Figure 5: The effective cross sections  $\sigma_2$  of the subprocess  $e\bar{b} \rightarrow \nu_e \bar{T}$  for the *LRTH* model(Fig.5a) and the *LHT* model(Fig.5b).

In Fig.5a we plot the cross section  $\sigma_2^{LR}$  for single production of the top partner  $T$  at the *THERA* with  $\sqrt{s} = 3.7$  TeV as a function of the scale parameter  $f$  for three values of the mixing parameter  $M$ . To compare single production of  $T$  at the *THERA* with that of the  $T$ -even top partner  $T_+$  predicted by the *LHT* model,  $\sigma_2^{LH}$  is shown in Fig.5b as a function of the scale parameter  $f$  for the mixing parameter  $x_L = 0.5$  and  $0.8$ . One can see from Fig.5 that the single production cross section of the top partner at the *THERA* is larger than that at the *ILC*. The cross section  $\sigma_2^{LH}$  is not sensitive to the free parameter  $x_L$  and its value is in the range of  $47.9$  fb  $\sim$   $0.19$  fb for  $x_L = 0.8$  and  $500$  GeV  $\leq f \leq 1000$  GeV. For  $100$  GeV  $\leq M \leq 300$  GeV and  $500$  GeV  $\leq f \leq 1000$  GeV, the value of  $\sigma_2^{LR}$  is in the range of  $72.7$  fb  $\sim$   $0.1$  fb. Thus, in most of the parameter space,  $\sigma_2^{LR}$  is larger than  $\sigma_2^{LH}$ .

For the dominating decay mode  $\phi^+ b$  of the top partner  $T$ , its single production can

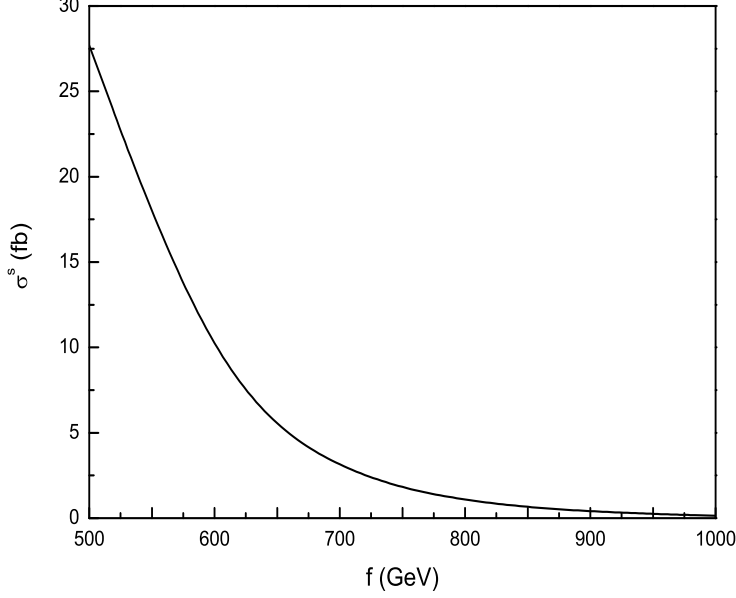


Figure 6: The production rate of the  $\nu_e \bar{t} b \bar{b}$  final state as a function of the parameter  $f$  for the mixing parameter  $M = 150 \text{ GeV}$ .

give rise to the  $\nu_e \bar{t} b \bar{b}$  final state, which is almost free of the  $SM$  background [23]. For the decay modes  $th$ ,  $tZ$ , and  $t\phi_0$ , if we assume that there are  $h \rightarrow b\bar{b}$ ,  $Z \rightarrow b\bar{b}$ , and  $\phi_0 \rightarrow b\bar{b}$ , the process  $ep \rightarrow \nu_e \bar{T} + X$  can also generate  $\nu_e \bar{t} b \bar{b}$  final state. The production rate of the  $\nu_e \bar{t} b \bar{b}$  final state can be easily estimated  $\sigma^s \approx \sigma_2 \times [Br(T \rightarrow \phi^+ b) \times Br(\phi^+ \rightarrow t\bar{b}) + Br(T \rightarrow th) \times Br(h \rightarrow b\bar{b}) + Br(T \rightarrow tZ) \times Br(Z \rightarrow b\bar{b}) + Br(T \rightarrow t\phi^0) \times Br(\phi^0 \rightarrow b\bar{b})]$ . The numerical results are shown in Fig.6. One can see from this figure that, with reasonable values of the free parameters of the  $LRT H$  model, the production rate can reach  $27 \text{ fb}$ . It is obvious that, for the decay channel  $T \rightarrow W^+ b$ , the mainly background of the process  $ep \rightarrow \nu_e \bar{T} + X$  comes from the  $SM$  process  $ep \rightarrow \nu_e \bar{t} + X$ , which has been extensively studied in Ref.[24]. The production rate of this kind of signal is too small to be separated from the large background.

For the  $T$ -even top partner  $T_+$  predicted by the  $LHT$  model, the decay modes  $W_H^+ b$

and  $B_H t$  make the process  $ep \rightarrow \nu_e \bar{T}_+$  generate the final state  $\bar{t} + X$ . Its dominating background is also the  $SM$  process  $ep \rightarrow \nu_e \bar{t} + X$ . In wide range of the parameter space of the  $LHT$  model, there are  $Br(Z_H \rightarrow B_H H) \simeq 1$ . In the case of  $H \rightarrow b\bar{b}$ , the decay modes  $Ht$  and  $Z_H t$  can give rise to similar signal to those of the decay modes  $\phi^+ b$ ,  $th$ ,  $tZ$  of the top partner  $T$ . However, its production rate is much smaller than that generated by the  $LRTH$  model. Thus, the possible signatures of the top partner  $T$  predicted by the  $LRTH$  model might be detected via the process  $ep \rightarrow \nu_e \bar{T} + X \rightarrow \nu_e \bar{t} b\bar{b} + X$  at the  $THERA$ , while it is not this case for the  $T$ -even top partner  $T_+$  predicted the  $LHT$  model.

## 5. Production of the top partner $T$ associated with the top quark $t$ at the $LHC$

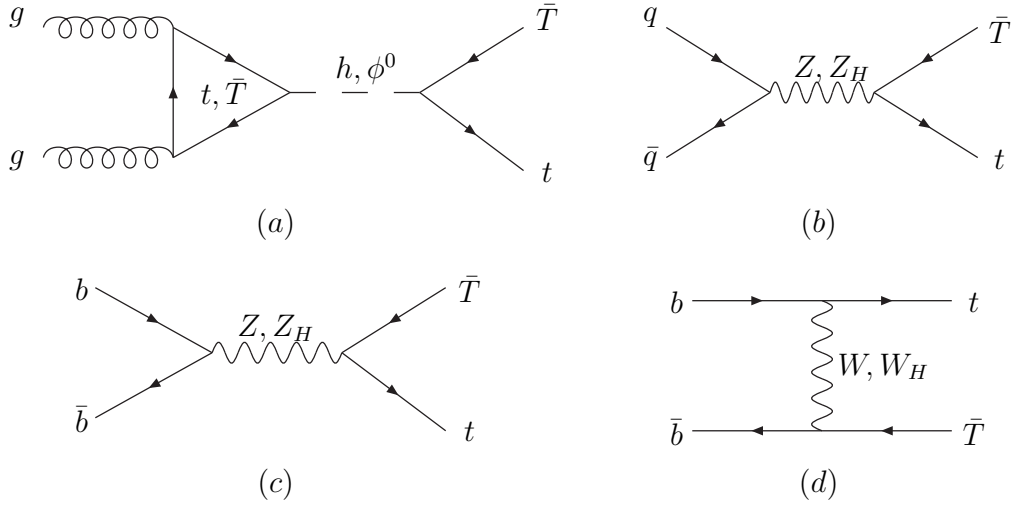


Figure 7: In the  $LRTH$  model, the *Feynman* diagrams for production of the top partner  $T$  associated with the top quark  $t$  at the  $LHC$ .

The  $LHC$  will soon go into full operation and provide proton-proton collisions at a *c.m.* energy  $\sqrt{s} = 14 \text{ TeV}$ . There are strong theoretical reasons to expect that the  $LHC$  will discover new physics beyond the  $SM$  up to  $TeV$ . At the  $LHC$ , the top partner can be pair-produced via  $QCD$  interactions and can be produced associated with a jet mediated by the  $SM$  gauge bosons, which have been extensively studied in the literature

[7, 9, 11, 25]. The top partner  $T$  can also be produced associated with the top quark  $t$  via the gluon fusion with neutral scalar exchanges and quark antiquark annihilation with the gauge boson exchanges. In the  $LRTH$  model, the *Feynman* diagrams for this kind of production processes are shown in Fig.7.

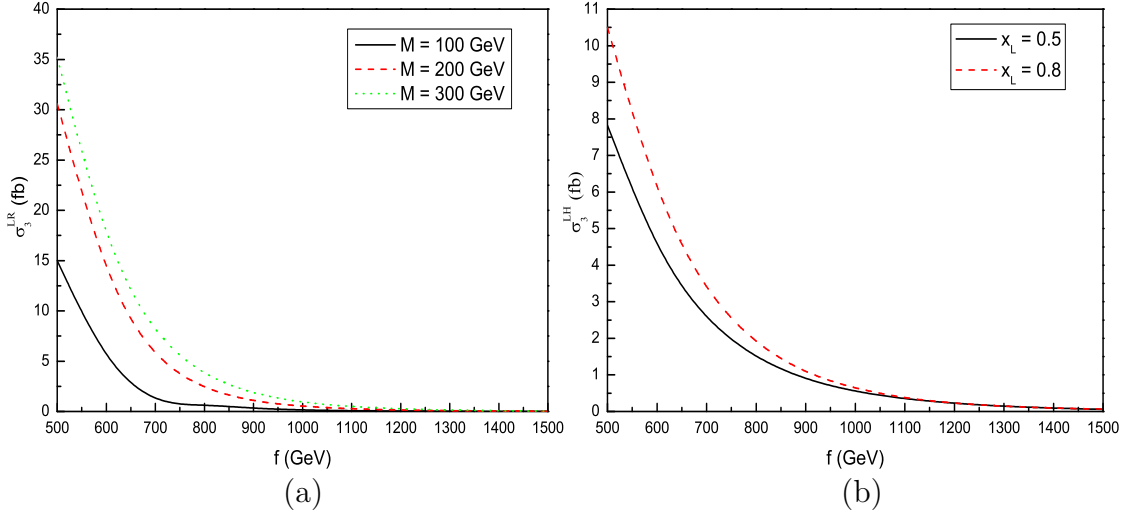


Figure 8: The hadronic cross sections  $\sigma_3$  for the subprocess  $gg \rightarrow t\bar{T} + \bar{t}T$  as function of the parameter  $f$  in the  $LRTH$  model (a) and the  $LHT$  model (b).

Similar with sections 3 and 4, using the relevant *Feynman* rules we can easily give the expressions of the parton level cross sections for the subprocesses  $q\bar{q} \rightarrow t\bar{T} + \bar{t}T$  ( $q = u, c, d$ , and  $s$ ) and  $b\bar{b} \rightarrow t\bar{T} + \bar{t}T$ . For the gluon-induced production of the top partner as shown in Fig.7a, we first obtain the effective couplings  $hgg$  and  $\phi^0 gg$  induced by the fermion loop, which have been extensively studied in the literature [26], then the parton level cross section  $gg \rightarrow t\bar{T} + \bar{t}T$  can be easily calculated. It is well known that the hadronic cross section can be obtained by folding the parton level cross section with the *PDFs* in the proton. Our numerical results are summarized in Fig.8 and Fig.9, in which Fig.8 and Fig.9 correspond to the subprocesses  $gg \rightarrow t\bar{T} + \bar{t}T$  and  $q\bar{q} \rightarrow t\bar{T} + \bar{t}T$  ( $q = u, c, d, s$ , and  $b$ ), respectively. The  $T$ -even top partner  $T_+$  predicted by the  $LHT$  model can also be produced in association with the top quark  $t$  at the  $LHC$ . The relevant *Feynman*

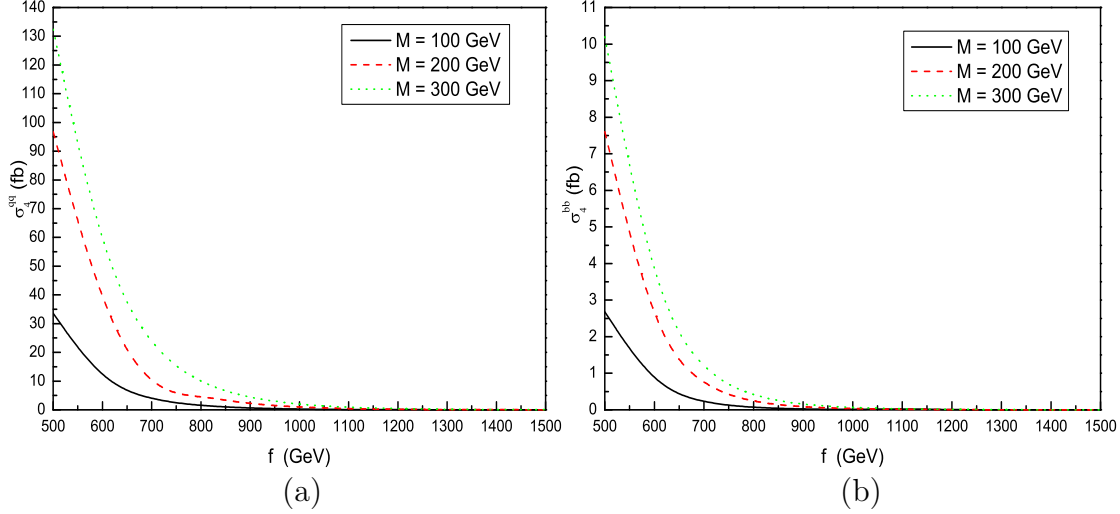


Figure 9: The hadronic cross sections  $\sigma_4$  for the subprocesses  $q\bar{q} \rightarrow t\bar{T} + \bar{t}T$ (a) and  $b\bar{b} \rightarrow t\bar{T} + \bar{t}T$ (b) as a function of the parameter  $f$  for three values of the mixing parameter  $M$ .

diagrams are similar with those of Fig.7. However, the new scalars and new gauge bosons predicted by the *LHT* model are *T*-odd, which have no contributions to the subprocesses  $gg \rightarrow t\bar{T} + \bar{t}T$  and  $q\bar{q} \rightarrow t\bar{T} + \bar{t}T$ . Thus, its production cross section induced by the gluon fusion mechanism is smaller than that of the top partner *T* as shown in Fig.8b. In most of the parameter space of the *LHT* model, the value of the hadronic cross section induced by the subprocess  $q\bar{q} \rightarrow t\bar{T} + \bar{t}T$  is smaller than  $5 \times 10^{-2} fb$ , so the relevant curve lines are not shown in Fig.9. One can see from these figures that, in the *LRTH* model, the hadronic cross section from the subprocess  $q\bar{q} \rightarrow t\bar{T} + \bar{t}T$  is larger than that from the subprocess  $gg \rightarrow t\bar{T} + \bar{t}T$ , while the contributions of the subprocess  $b\bar{b} \rightarrow t\bar{T} + \bar{t}T$  to the hadronic cross section should not be neglected. For  $100 GeV \leq M \leq 300 GeV$  and  $500 GeV \leq f \leq 1500 GeV$ , the value of the total hadronic cross section is in the range of  $177.6 fb \sim 0.013 fb$ . If we assume the yearly integrated luminosity  $\mathcal{L}_{int} = 100 fb^{-1}$  for the *LHC* with the *c.m.* energy  $\sqrt{s} = 14 TeV$ , then there will be several up to ten thousands of the  $t\bar{T} + \bar{t}T$  events to be generated per year.



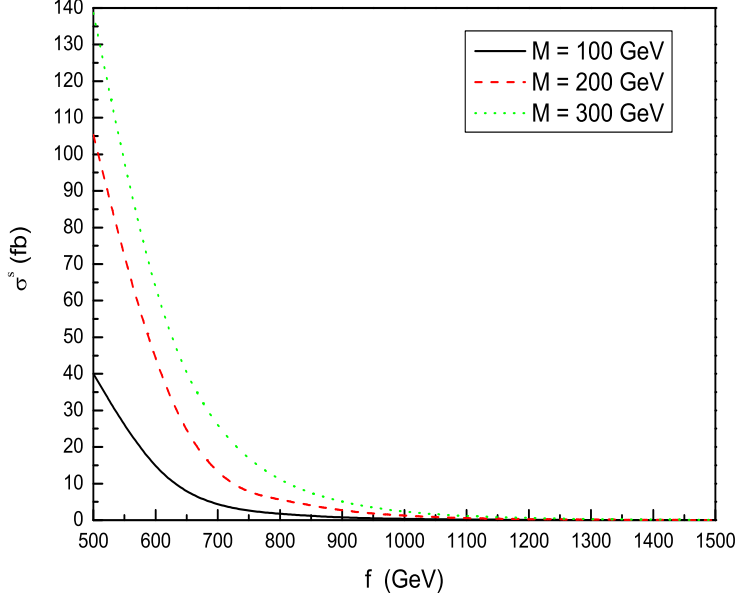


Figure 10: In the  $LRTH$  model, production rate for the  $t\bar{t}b\bar{b}$  final state as a function of the parameter  $f$  for three values of the mixing parameter  $M$ .

From the discussions given in section 3, the decay modes  $\phi^+b$ ,  $ht$ ,  $Zt$ , and  $\phi^0t$  of the top partner  $T$  with  $h \rightarrow b\bar{b}$ ,  $Z \rightarrow b\bar{b}$  and  $\phi^0 \rightarrow b\bar{b}$  can make the process  $pp \rightarrow t\bar{T} + \bar{t}T + X$  give rise to the  $t\bar{t}b\bar{b}$  final state. Its production rate is plotted in Fig.10 as a function of the parameter  $f$  for three values of the mixing parameter  $M$ . One can see that, with reasonable values of the free parameters, the production rate can be larger than  $100fb$ . However, its value decreases quickly as the parameter  $f$  increasing. The main backgrounds for the  $t\bar{t}b\bar{b}$  final state come from the  $SM$  processes  $PP \rightarrow t\bar{t}Z + X$  and  $PP \rightarrow t\bar{t}h + X$  with  $Z \rightarrow b\bar{b}$  and  $h \rightarrow b\bar{b}$ , continuum  $t\bar{t}b\bar{b}$  production, and the reducible background  $t\bar{t} + jets$ , in which the additional jets light quarks or gluons but may be misidentified as  $b$  quarks. Detailed analysis of the signals and the relevant backgrounds have been given in Ref.[27]. They have shown that the most large background  $t\bar{t} + jets$  can be suppressed by enhancing the detector ability to tag  $b$  quark jets. Furthermore, It may be help to

distinguish the  $t\bar{t}b\bar{b}$  final state from the second large background coming from the process  $PP \rightarrow t\bar{t}h + X$  by calculating the invariant mass of the  $tb\bar{b}$  state generated by the top partner  $T$  decaying. Thus, it may be possible to extract the signals from the backgrounds by applying suitable cuts. Certainly, detailed confirmation of the observability of the signals generated by the process  $pp \rightarrow t\bar{T} + \bar{t}T + X$ , would require Monte-Carlo simulations of the signals and backgrounds, which is beyond the scope of this paper. It is obvious that it is more difficult to separate the signals generated by the process  $pp \rightarrow t\bar{T} + \bar{t}T + X$  with  $T \rightarrow W^+b$  from the large background coming from the  $SM$  process  $pp \rightarrow t\bar{t} + X$ . Certainly, the reconstruction of the heavy top partner  $T$  through the combination of  $Wb$  may help to distinguish the signals from the backgrounds.

## 6. Conclusions

The twin *Higgs* mechanism provides an alternative method to solve the little hierarchy problem. The *LRTH* model is a concrete realization of the twin *Higgs* mechanism, which predicts the existence of the top partner  $T$ . In this paper, we consider production of  $T$  associated with the top quark  $t$  in future *ILC* and *LHC* experiments, and its single production in future *THERA* experiments. To compare our results obtained in the context of the *LRTH* model with those of the *LHT* model, we also estimate production of the  $T$ -even top prater  $T_+$  via the corresponding processes in these high energy collider experiments. From our numerical results, we can obtain the following conclusions.

i) In most of the parameter space, the production cross sections of the top partner  $T$  are larger than those of the  $T$ -even top partner  $T_+$  in these three kinds of collider experiments. However, all of their values decrease quickly as the parameter  $f$  increasing.

ii) In the context of the *LHT* model, the production cross section of the process  $pp \rightarrow t\bar{T} + \bar{t}T + X$  is larger than that of the process  $e^+e^- \rightarrow t\bar{T} + \bar{t}T$  or the process  $ep \rightarrow \nu_e\bar{T} + X$ . For  $100 \text{ GeV} \leq M \leq 300 \text{ GeV}$  and  $500 \text{ GeV} \leq f \leq 1500 \text{ GeV}$ , the value of the production cross section for the process  $pp \rightarrow t\bar{T} + \bar{t}T + X$  is in the range of  $177.6 \text{ fb} \sim 0.013 \text{ fb}$ .

iii) The decay modes of the top partner  $th, tZ$ , and  $t\phi_0$ , with  $h \rightarrow b\bar{b}$ ,  $Z \rightarrow b\bar{b}$ , and  $\phi_0 \rightarrow b\bar{b}$  can give rise to similar signals with those of the decay modes  $\phi^+b$ . They can

produce the  $\nu_e \bar{t} b \bar{b}$  and  $t \bar{t} b \bar{b}$  final states in the *THEHA* and *LHC* experiments, respectively. Although the production rate of the  $\nu_e \bar{t} b \bar{b}$  final state is smaller than that of the  $t \bar{t} b \bar{b}$  final state, the  $\nu_e \bar{t} b \bar{b}$  final state is more easy detected because of it almost free of the *SM* backgrounds [23]. Considering the very large backgrounds, the decay channel  $T \rightarrow W^+ b$  can not be used to detecting the possible signals of the top partner  $T$  in future high energy collider experiments.

## Acknowledgments

This work was supported in part by the National Natural Science Foundation of China under Grants No.10675057, Specialized Research Fund for the Doctoral Program of Higher Education(SRFDP) (No.200801650002), the Natural Science Foundation of the Liaoning Scientific Committee(No.20082148), and Foundation of Liaoning Educational Committee(No.2007T086).

## References

- [1] R. Barbieri and A. Strumia, *Phys. Lett. B***462**(1999)144.
- [2] H. P. Nilles, *Phys. Rept.* **110**(1984)1; H. E. Haber and G. L. Kane, *Phys. Rept.* **117**(1985)75.
- [3] For review, see: M. Schmaltz and D. Tucker-Smith, *Annu. Rev. Nucl. Part. Sci.* **55**(2005)229; M. Perelstein, *Prog. Part. Nucl. Phys.* **58**(2007)247.
- [4] I. Antoniadis, *Phys. Lett. B***246**(1990)377; T. Appelquist, H. C. Cheng and B. A. Dobrescu, *Phys. Rev. D***64**(2001)035002.
- [5] Z. Chacko, H.-S. Goh and R. Harnik, *Phys. Rev. Lett.* **96**(2006)231802; Z. Chacko, Y. Nomura, M. Papucci and G. Perez, *JHEP* **0601**(2006)126; R. Foot and R. R. Volkas,

- Phys. Lett. B***645**(2007)75; A. Falkowski, S. Pokorski and M. Schmaltz, *Phys. Rev. D***74**(2006)035003; S. Chang, L. J. Hall and N. Weiner, *Phys. Rev. D***75**(2007)035009.
- [6] P. H. Frampton, P. Q. Hung, M. Sher, *Phys. Rep.* **330**(2000)263.
- [7] J. A. Aguilar-Saavedra, *Phys. Lett. B***625**(2005)234 [Erratum: *Phys. Lett. B***633**(2006)792]; G. Azuelos et al., *Eur. Phys. J. C***39S2**(2005)13; P. Meade, M. Reece, *Phys. Rev. D***74**(2006)015010; B. Holdom, *JHEP* **0703**(2007)063; R. Contino, G. Servant, *JHEP*. **0806**(2008)026; Tao Han, R. Mahbubani, D. G. E. Walker, Lian-Tao Wang, *arXiv*: **0803. 3820**[hep-ph].
- [8] K. Kong, S. C. Park, *JHEP* **0708**(2007)038; J. M. Cabarcas, D. G. Dumm, R. Martinez, *Eur. Phys. J. C***58**(2008)569; Chong-Xing Yue, Li-Hong Wang, Jia Wen, *Chin. Phys. Lett.* **25**(2008)1613.
- [9] Kingman Cheuing, C. S. Kim, Kang Young Lee, and Jeonghyon Song, *Phys. Rev. D***74**(2006)115013; M. S. Carena, J. Hubisz, M. Perelstein, *Phys. Rev. D***75**(2007)091701; G.-H. Cao, Chong-Sheng Li, C.-P. Yuan, *Phys. Lett. B***668**(2008)24; S. Matsumoto, M. M. Nojiri, D. Nomura, *Phys. Rev. D***75**(2007)055006; D. Choudhury, D. K. Ghosh, *JHEP* **0708**(2007)084; M. M. Nojiri, M. Takeuchi, *JHEP* **0810**(2007)025; S. Matsumoto, T. Moroi, K. Tobe, *Phys. Rev. D***78**(2008)055018; G. H. Brooijmans et al [Non SUSY New Physics Working Group], *arXiv*: **0802. 3715**[hep-ph].
- [10] Z. Chacko, H.-S. Goh and R. Harnik, *JHEP* **0601**(2006)108.
- [11] H.-S. Goh and S. Su, *Phys. Rev. D***75**(2007)075010.
- [12] A. Abada, I. Hidalgo, *Phys. Rev. D***77**(2008)113013; Y.-B. Liu, H.-M. Han, X.-L. Wang, *Eur. Phy. J. C***53**(2008)615.
- [13] Dong-Won Jung and Jae Yong Lee, *arXiv*: **0710. 2589**[hep-ph].
- [14] E. M. Dolle, S. Su, *Phys. Rev. D***77**(2008)075013.

- [15] H. C. Cheng, I. Low, *JHEP* **0309**(2003)051; *JHEP* **0408**(2004)061; I. Low, *JHEP* **0410**(2004)067.
- [16] W.-M. Yao et al. [Particle Data Group], *J. Phys. G***33**(2006)1 and partial update for the 2008 edition.
- [17] S. Moretti, *Phys. Lett. B***452**(1999)338; H. Baer, S. Dawson, L. Reina, *Phys. Rev. D***61**(2000)013002; C. Schwinn, *hep-ph/0412028*; K. Kolodziej, S. Szczypinski, *Acta Phys. Polon. B***38**(2007)3609; K. Kolodziej, S. Szczypinski, *Nucl. Phys. B***801**(2008)153.
- [18] K. Hagiwara, H. Murayama and I. Watanabe, *Nucl. Phys. B***367**(1991)257; B. Grzadkowski, J. Pliszka, *Phys. Rev. D***60**(1999)115018; A. Gay, *Eur. Phys. J. C***49**(2007)489; Dai Lei, Ma Wen-Gan, Zhang Ren-You, Guo Lei, and Wang Shao-Ming, *Phys. Rev. D***78**(2008)094010.
- [19] A. Belyaev, Chuan-Ren Chen, K. Tobe, C.-P. Yuan, *Phys. Rev. D* **74**(2006)115020.
- [20] J. Hubisz, P. Meade, *Phys. Rev. D***71**(2005)035016.
- [21] S. Sultansay, *Eur. Phys. J. C***33**(2004)S1064 and references therein.
- [22] J. Pumplin et al. (CTEQ Collaboration), *JHEP* **02**(2006)032.
- [23] K. Cheung, *Phys. Lett. B***319**(1993)244; G. A. Leil, S. Moretti, *Phys. Rev. D***53**(1996)163; *D***53**(1996)178.
- [24] S. Moretti, K. Odagiri, *Phys. Rev. D***57**(1998)3040.
- [25] Tao. Han, H. E. Logan, B. McElrath, and Lian-Tao Wang, *Phys. Rev. D***67**(2003)095004.
- [26] For example see: L. Reina, *hep-ph/0512377*.
- [27] J. Dai, J. F. Gunion, R. Vega , *Phys. Rev. Lett.***71**(1993)2699; J. Goldstein, et al., *Phys. Rev. Lett.* **86**(2001)1694.